CCFE-PR(15)63

Lavrentiev M Yu, Wróbel J S, Nguyen-Manh D, Dudarev S L,
Ganchenkova M G, L.W. G. Morgan and D.Kotlyar

Magnetic Cluster Expansion model for random and ordered magnetic face-centered cubic Fe-Ni-Cr alloys

Magnetic Cluster Expansion model for random and ordered magnetic face-centered cubic Fe-Ni-Cr alloys

M.Y. Lavrentiev[1], J.S. Wróbel[1], D. Nguyen-Manh[1], S.L. Dudarev[1], and M.G. Ganchenkova[2]

[1]CCFE, Culham Science Centre, Abingdon, Oxon, OX14 3DB, UK

[2]Materials Science Department, National Research Nuclear University MEPhI, 31 Kashirskoe sh., 115409, Moscow, Russia

Magnetic Cluster Expansion model for random and ordered magnetic face-centered cubic Fe-Ni-Cr alloys

M.Y. Lavrentiev[(1)], J.S. Wróbel[(1)], D. Nguyen-Manh[(1)], S.L. Dudarev[(1)], and M.G. Ganchenkova[(2)]

(1) CCFE, Culham Science Centre, Abingdon, Oxon, OX14 3DB, UK
(2) Materials Science Department, National Research Nuclear University MEPhI, 31 Kashirskoe sh., 115409, Moscow, Russia

Abstract

Using density functional theory (DFT) calculations, we develop a Magnetic Cluster Expansion (MCE) model for ternary face-centered cubic Fe-Ni-Cr alloys. Parameters of the MCE Hamiltonian are derived from DFT calculations spanning binary and ternary alloy systems. Using the MCE Hamiltonian, we perform Monte Carlo simulations and model magnetic structures of alloys over the entire range of alloy compositions for both random and ordered alloy structures. In random alloys, the removal of magnetic collinearity constraint reduces the total magnetic moment, but it does not affect the predicted range of compositions where alloys adopt ferromagnetic low temperature configurations. During alloying of ordered fcc Fe-Ni compounds, chromium atoms tend to replace nickel rather than iron atoms. Replacement of Ni by Cr in alloys with high iron content increases the Curie temperature of the alloys. This can be explained by strong antiferromagnetic Fe-Cr coupling, similar to that found in bcc Fe-Cr solutions, where the increase of the Curie temperature, predicted by simulations as a function of Cr concentration, agrees with what is found experimentally.

I. Introduction

Fe-Cr-Ni based austenitic stainless steels retain high mechanical strength at elevated temperatures, making them attractive structural materials for light water and fast breeder fission reactors [1]. Also, because of its robustness, austenitic stainless steel 316L(N) was selected for ITER [2]. Until now, very few theoretical investigations of this ternary alloy system were performed, owing to the difficulty of treating the interplay between structural order and magnetism in these materials. Recently, we have developed an *ab initio* parameterized Heisenberg–Landau Hamiltonian based Magnetic Cluster Expansion (MCE) lattice model for binary fcc Fe–Ni [3]. To describe the high- *and* low-spin magnetic configurations of fcc Fe, terms up to the 8^{th} order in magnetic moment had to be included in the Landau expansion for the on-site magnetic energy. Thermodynamic and magnetic properties of the alloys were explored using configurational and magnetic Monte Carlo simulations over a broad temperature range extending well over 1000 K. The predicted fcc-bcc coexistence curve, the phase stability of ordered Fe_3Ni, FeNi, and $FeNi_3$ intermetallic compounds, and the predicted temperatures of magnetic transitions simulated as functions of alloy compositions, were found to agree well with experimental observations. In particular, simulations show that magnetic interactions stabilize fcc phases of binary Fe–Ni alloys. Parameters of the MCE model were derived from DFT calculations performed for a large number of representative atomic configurations, as well as from DFT data on pure fcc metals. The success of the MCE model for Fe-Ni, together with a recent comprehensive *ab initio* investigation of ternary Fe-Ni-Cr alloys [4], makes it desirable to extend MCE to the ternary fcc Fe-Ni-Cr alloy system.

Ternary Fe-Ni-Cr system is the first example of application of the Magnetic Cluster Expansion to an alloy containing more than two components. Initial parameterization of the Fe-Ni-Cr MCE Hamiltonian and a limited amount of simulations are given in Ref. [4]. Here we develop an improved fit based on a larger DFT database of structures and magnetic configurations. Monte Carlo simulations using the MCE Hamiltonian describe both random and ordered alloy structures. Advantages of MCE include the possibility of treating a broad range of alloy compositions and a large variety of chemical and magnetic configurations. Also, the method makes it possible to study magnetic properties of both ferro- and antiferromagnetic alloys. This aspect of the model is particularly significant in relation to fcc Fe-Ni-Cr alloys, since Ni at low temperature is ferromagnetic, whereas pure fcc Fe and Cr, according to *ab initio* calculations, have vanishing total magnetic moments.

II. Magnetic Cluster Expansion model for a Ternary Alloy

MCE has been applied to a number of binary alloy systems, including bcc and fcc Fe-Cr [5] and fcc Fe-Ni [3]. Combining MCE with experimental data on vibrational spectra we explained the origin of bcc-fcc structural phase transitions in pure Fe and reproduced the fcc γ-loop in the Fe-Cr phase diagram. In the case of Fe-Ni alloys, a phase diagram including both disordered alloy configurations and ordered FeNi and $FeNi_3$ compounds was derived [3]. A large DFT database of atomic structures and magnetic configurations generated as a part of a recent investigation of Fe-Ni-Cr alloys [4] now makes it possible extend Magnetic Cluster Expansion treatment of fcc Fe-Ni system to the ternary alloy case. Within the MCE formalism [6,7], each alloy configuration is defined by both its chemical (σ_i) and magnetic ($\mathbf{M}_i$) atomic degrees of freedom. To simplify applications of MCE to ternary alloys and reduce the number of model parameters, the ternary alloy MCE Hamiltonian includes only pairwise interatomic interactions. The energy of an arbitrary structural and magnetic alloy configuration $\left(\{\sigma_i\},\{\mathbf{M}_i\}\right)$ in MCE has the form:

$$
\begin{aligned}
E\left(\{\sigma_i\},\{\mathbf{M}_i\}\right) &= \sum_{ij\in 1NN} I^{(1NN)}_{\sigma_i\sigma_j} + \sum_{ij\in 2NN} I^{(2NN)}_{\sigma_i\sigma_j} + \ldots \\
&+ \sum_i A_{\sigma_i}\mathbf{M}_i^2 + \sum_i B_{\sigma_i}\mathbf{M}_i^4 + \sum_i C_{\sigma_i}\mathbf{M}_i^6 + \sum_i D_{\sigma_i}\mathbf{M}_i^8 + \\
&\sum_{ij\in 1NN} Y^{(1NN)}_{\sigma_i\sigma_j}\mathbf{M}_i\cdot\mathbf{M}_j + \sum_{ij\in 2NN} Y^{(2NN)}_{\sigma_i\sigma_j}\mathbf{M}_i\cdot\mathbf{M}_j + \ldots ,
\end{aligned}
\qquad (1)
$$

where σ_i, σ_j = Fe, Cr, or Ni, $\mathbf{M}_i$ is the magnetic moment of atom *i*, and the non-magnetic and magnetic interaction parameters (I_{ij} and Y_{ij}, respectively) for each interatomic separation in the lattice are 3×3 matrices defined in the discrete space of atomic species. Parameters *A*s, *B*s, *C*s and *D*s represent Landau coefficients for the quadratic, quartic 6th and 8th order magnetic self-energy terms, respectively. To make the model consistent with the MCE Hamiltonian for Fe-Ni alloys, it uses the 29 binary fcc Fe-Ni configurations that were used for fitting the model and applying it to fcc Fe-Ni alloys [3]. The magnetic Fe-Fe and Ni-Ni interaction parameters are retained from the Fe-Ni MCE parameterization, whereas the possibility of modifying the Fe-Ni interaction parameters has been included in the new fit. In addition to binary Fe-Ni configurations, the new parameterization is based on the DFT data for the 31 ordered ternary Fe-Cr-Ni structures spanning the entire alloy composition triangle, together with the DFT data on pure elements. Note that no Ni-Cr binary structures were used in the fitting, so that the results obtained for systems with low iron content are expected to be less accurate than those for iron-rich compounds. *Ab*

initio calculations were performed using the projector augmented wave method implemented in VASP package. Similarly to the binary Fe-Ni case, interactions were assumed to extend up to the fourth nearest neighbor in the fcc lattice, so that altogether the model involves 24 non-magnetic (I_{ij}) and 24 magnetic (Y_{ij}) interaction parameters. At the first stage of fitting, the on-site terms *A*, *B* etc. were fitted using the energy versus magnetic moment curves computed for ferromagnetic pure Fe, Ni, and Cr. For chromium, only quadratic and quartic terms in the Landau expansion for the energy versus magnetic moment were used, whereas for iron and nickel the on-site Landau expansion was extended to the 8^{th} order in magnetic moment. The dependence of the on-site energy terms on the environment was neglected to reduce the number of model parameters. Subsequently, using the procedure described in [3], fitting of interaction terms *I* and *Y* was performed for both energies and magnetic moments on each atom in the simulation cell. The average error of the fit is 18 meV/atom. A complete list of interatomic MCE interaction parameters for Fe-Cr-Ni alloys is given in the Table 1. The on-site terms are given in Table 2.

To check the accuracy of MCE fit for magnetic moments, we selected several special quasi-random structures (SQS) with Fe content close to 70 at. %, Cr content close to 18 at. %, and Ni content close to 12 at. %. The structures comprised 108 atoms each, corresponding to 27 (3×3×3) fcc unit cells. Magnetic moments of atoms in these structures were calculated in the collinear approximation using both DFT and MCE. MCE simulations were performed in two different ways, with and without the collinearity constraint on the direction of magnetic moments. Table 3 compares the results obtained using the two approaches. In the case of MCE simulations performed under the collinearity constraint, the two approaches agree well for the four out of five structures studied. Once the collinearity requirement was removed, magnetic moments rotated away from their magnetization axis, and the total moment of the system decreased. Also, the moments of individual atomic species decreased. The non-collinear magnetic configurations were found to be more stable than collinear configurations, although the energy gain associated with the relaxation of collinear magnetic states into non-collinear ones was relatively small, from 3 to 11 meV/atom, which is within the accuracy of the fit; so it is not possible to conclude unambiguously whether the true ground state is collinear or not.

Most of the structures used in the parameterization of Hamiltonian (1) belonged to the Fe-rich area of the ternary phase diagram and to Fe-Ni solid solutions. Hence we expect that predictions derived from MCE simulations should be more reliable for alloys where Fe content exceeded 50 at %, as well as for alloys where Fe and Ni were the dominant components. Almost all the Monte Carlo simulations were performed using 16384 atom simulation cells (containing 16×16×16 fcc unit cells). Each Monte Carlo run included

80000 attempts to change magnetic moment per atom at the equilibration stage, and subsequently the same number of attempts at the accumulation stage. As an example of application of MCE to low-temperature magnetic properties of a ternary alloy system, we investigated the dependence of the total magnetic moment of $(Fe_{0.5}Ni_{0.5})_{1-x}Cr_x$ alloy on Cr content. This was also investigated by DFT in [4]. It was found in [4] that the average magnetic moment of the alloy decreased rapidly as a function of chromium content. In the MCE Monte Carlo simulations, an ordered FeNi system with $L1_0$ structure was chosen as the initial configuration. The total magnetic moment per atom was found to be 1.606 μ_B, close to the DFT value of 1.63 μ_B. Chromium content was then increased by replacing an equal number of Fe and Ni atoms in their corresponding sub-lattices with Cr atoms, with positions of chromium atoms being chosen at random. With increasing Cr content, magnetization rapidly decreases, resulting in a completely non-magnetic alloy at x_{Cr}=0.4, in agreement with *ab initio* DFT results.

III. Random Fe-Ni-Cr Mixtures

Technologically important Fe-Ni-Cr austenitic steels [1,2,8] are usually produced at high temperatures (1000° C and more [9]) and with reactor operating temperatures of over 0.3 T_m, where T_m is the alloy melting temperature and high irradiation doses [10], their structure is close to a completely random solid mixture. For example, in almost all the experimentally investigated binary Fe-Cr, Fe-Ni, and ternary Fe-Ni-Cr alloys [11-18], the magnitude of short-range order parameters does not exceed 0.1 for all the three pairs of elements. Thus, a completely random ternary solid solution approximation provides a good representation of a real alloy.

A search for magnetic ground states was performed over the entire range of alloy compositions. The concentration step for each element was 6.25 at. %. Three-stage magnetic quenching was performed, from temperature T=1000 K to T=1 K (first stage), then down to 10^{-3} K (second stage), and finally to 10^{-6} K (third stage). Pure fcc Fe and Cr were found to have vanishing total magnetic moments, in agreement with DFT results. Experimental studies of coherent Fe precipitates in fcc Cu matrix show that the magnetic ground state of fcc Fe is non-collinear [19,20], whereas in fcc Cr non-magnetic ground state was found in DFT calculations [4]. Our MCE Hamiltonian simulations predict non-collinear ground state for Fe, while for the fcc Cr collinear antiferromagnetic ground state was found, which is only 6 meV/atom more favourable energetically than the non-magnetic state. Pure fcc Ni is predicted as collinear ferromagnetic, also in agreement with experiment. As a result, random structures with nonzero total magnetic moment are mostly found in the Ni-rich part of alloy composition triangle. Figure 2 shows the total magnetic

moment at T → 0 K (ground state) as a function of alloy composition found in simulations performed with and without the collinearity constraint. In both cases the addition of up to 50 at. % of Fe or Cr to pure nickel increases the overall magnetic moment per atom and the alloy remains ferromagnetic. While for the Fe-Ni alloy this agrees very well with the *ab initio* data [4], for the Ni-Cr system rapid decrease of the magnetic moment was found both in DFT [4] and experimental studies [21], with vanishing total moment above 20 at. % Cr. This disagreement is related to the already mentioned fact that no Ni-Cr binary structures were used in the fitting, so that the results obtained for systems with low iron content are less accurate than those for iron-rich compounds. At higher concentrations of Fe or Cr, the moment in MCE simulations decreases sharply and alloys become antiferromagnetic if less than 25 at. % Ni remains. Collinear constraint leads to the overall increase of average magnetic moment, but the areas in the ternary concentration triangle where the moment is nonzero largely coincide, including an interval at the Fe-Cr line. The occurrence of such an interval stems from antiferromagnetic coupling between Fe and Cr, which results in the non-compensated total moment if the iron content exceeds that of chromium. It is instructive to compare Figure 2 with Figure 9 of [4], where moments of the most stable ordered Fe-Ni-Cr systems are shown. Regions corresponding to non-zero magnetic moment are very similar, but the magnitude of the moment is higher for the ordered stable structures compared with random structures, reaching almost 2 μ_B at the Fe-Ni line.

When analysing the energies characterising Fe-Ni-Cr alloys, it is important to distinguish between the enthalpy of mixing and enthalpy of formation. The difference between them stems from the fact that for pure Ni, fcc structure has the lowest energy, while for Fe and Cr, bcc phases are more stable energetically. The enthalpy of mixing of fcc Fe-Ni-Cr is calculated with respect to the enthalpies of constituting elements assuming that they all have fcc crystal structure. The enthalpy of formation, on the other hand, is calculated with respect to the lowest energy structures. A comprehensive *ab initio* study of different structures was performed in [4], and in the current work we use the fcc-bcc energy differences derived there, namely, E_{fcc}(Fe)-E_{bcc}(Fe) = 82 meV/atom; E_{fcc}(Cr)-E_{bcc}(Cr) = 405 meV/atom; E_{fcc}(Ni)-E_{bcc}(Ni) = −96 meV/atom. Enthalpies of mixing and formation for fcc Fe-Ni-Cr alloys at T → 0 K are shown in Figure 3. The mixing enthalpy is negative over the entire range of alloy compositions, with the lowest absolute values corresponding to the Ni-Cr binary mixture (note that these are values characterising random mixtures only). The enthalpy of formation is minimum near the pure Ni corner of the phase diagram.

At high temperatures, magnetic order vanishes for almost all the alloy compositions already at temperatures close to T=500 K (see Figure 4). Ferromagnetism is retained only in the Ni-rich corner of

the phase diagram. This agrees with our previous simulations [3] showing that magnetic order in pure Ni, as predicted by the present MCE Hamiltonian, vanishes at 550-600 K (the experimental Curie temperature of nickel is 631 K [22]). It is interesting to note that there is also another region where high-temperature magnetic order persists, namely in random Fe-Cr mixtures with composition from Fe_2Cr to Fe_3Cr (Figure 4). The reason for the occurrence of high-temperature magnetic order here (as well as large magnetic moment at low temperatures, see Figure 2) is related to strong first nearest neighbour antiferromagnetic interaction between Fe and Cr (Table 1). This produces an effect similar to the one responsible for the Curie temperature of bcc Fe-Cr alloys being maximum at 6 at % Cr [23], although in the case of fcc alloys ferromagnetism emerges in a mixture of two *antiferromagnetic* metals. The emergence of ferromagnetic order here was also noted in DFT studies [4].

IV. Ordered Fe-Ni-Cr Structures

Magnetic properties of several ordered Fe-Ni and Fe-Ni-Cr compounds were also investigated using the MCE-based Monte Carlo simulations. The phase diagram of binary Fe-Ni alloys involves two, or possibly three, ordered stoichiometric compounds, namely FeNi with $L1_0$ structure, $FeNi_3$ and Fe_3Ni with $L1_2$ structure. While $FeNi_3$ is a well-known compound and FeNi (tetrataenite) is found in meteorites [24-26], Fe_3Ni is an assumed compound, since it is less stable compared to a random Fe-Ni alloy of the same composition than the two other compounds.

Having completed the investigation of binary Fe-Ni compounds [3], we now pose a question about how the addition of chromium influences their energy and magnetic properties. For example, it is desirable to clarify which of the two elements, Fe or Ni, is more readily replaced by chromium. To answer this question, we performed Monte Carlo simulations of all the three above stoichiometric compounds with chromium atoms replacing either Fe or Ni, or both Fe and Ni (equal number of atoms of each species). The fcc lattice sites where Cr atoms replaced Fe or Ni atoms were chosen at random. Figures 5 (a-c) show the low-temperature enthalpy of the three compounds plotted as a function of Cr content. Cr concentration varied from 0 to 25 at % for $FeNi_3$ and Fe_3Ni, and from 0 to 50 at. % for FeNi. In all the three cases, chromium atoms clearly prefer Ni sites for replacement, with enthalpy difference being as high as 50 meV/atom. The tendency of Cr to replace Ni rather than Fe can be explained by strong Fe-Cr antiferromagnetic interaction in the first nearest neighbor configuration and by larger magnetic moment of chromium compared to nickel (note that in Hamiltonian (1), the energy of magnetic interaction is a sum of products of interaction parameters and scalar products of magnetic moments, and not the moment

unit vectors as in some of Heisenberg Hamiltonians). It is also reasonable to expect that strong magnetic Fe-Cr interaction might also influence the Curie temperature of the alloy. To investigate this, temperature-dependent Monte Carlo simulations were performed for all these compounds, with 1024 Cr atoms (6.25 at. %) added to the simulation cell, again randomly replacing Fe, Ni, or both Fe and Ni (512 atoms of each species). Figure 6 shows the temperature dependence of the total magnetic moment. For all the three compounds, the addition of Cr results in the reduction of the total magnetic moment of the system. The presence of Cr also changes the Curie temperature of all the systems, but it is in Fe_3Ni where this change is the largest. Here, the addition of Cr to Ni sites increases the temperature of magnetic transition from ~500 K to well over 700 K. The replacement of both Fe and Ni atoms with Cr also increases the T_C, while adding Cr to only Fe sites does not have such an effect (Figure 6a). For the $L1_0$ FeNi compound, the replacement of Ni by Cr results in the increase of the Curie temperature by less than 100K, while in the $FeNi_3$, all the possible substitutions of atoms with Cr lead to the decrease of the T_C. We interpret this finding as related to the ferromagnetic first, third and fourth nearest neighbour Ni-Cr interactions (see Table 1), which are weaker than ferromagnetic Ni-Ni interactions. As a result, in the Ni-rich systems the replacement of Ni with Cr results in the decrease of the T_C, as opposed to the Fe-rich systems. It is important to note here that the effect of Curie temperature increase has already been found experimentally in bcc Fe-Cr alloys with small (below 10 at. %) chromium content [22,27] and explained by strong antiferromagnetic Fe-Cr interactions using MCE simulations [22]. An experimental study of disordered fcc $(FeNi)_{1-x}Cr_x$ alloys for x = 0, 5, 10, and 15 at. % was performed in [28] and has shown substantial decrease of the Curie temperature with increasing chromium content (from almost 800 K for x = 0 down to under 200 K for x = 15 %). The authors of [28] also note appreciable distribution of magnetic ordering temperatures for 10 and 15 at. % Cr. Comparison of their results for T_C with our simulations for both ordered $L1_0$ FeNi and completely random Fe-Ni system with Cr replacing both iron and nickel may suggest transition from ordered FeNi to random Fe-Ni-Cr alloy with increasing chromium content in the experimental study. It would be very interesting to perform a new investigation of magnetic properties of ordered and random FeNi systems with controlled Cr replacement on each of the species or on both of them.

We also investigated the ternary ordered alloy Fe_2NiCr. The crystal structure of Fe_2NiCr is similar to $L1_0$ FeNi, with one of the Ni atoms replaced with Cr in each unit cell. This structure was extensively studied using *ab initio* methods [4] and was found to have lower enthalpy of mixing than all the experimentally known intermetallic phases in fcc Fe-Ni-Cr system. Initial MCE investigation of this alloy was performed in [4], but because of the significance of the Fe_2NiCr compound, we simulated its properties again using the improved MCE fit. Our simulations for the ground states of random and ordered Fe_2NiCr are

summarized in Table 4, together with the DFT calculations [4]. Ordered Fe_2NiCr was found to have almost exactly collinear magnetic structure. While our results show that a random mixture with atomic content $Fe_{50}Ni_{25}Cr_{25}$ is almost completely antiferromagnetic (the average magnetic moment is 0.025 μ_B per atom with no collinearity constraint, and 0.206 μ_B per atom with collinearity constraint applied), an ordered structure with the same composition has large nonzero total magnetic moment, with Cr moments being antiferromagnetically ordered with respect to the Fe moments. Its mixing enthalpy was found to be -233 meV/atom, which is lower than the mixing enthalpy of any of the random mixtures (see Figure 3(a)), and significantly lower than the value of -153 meV/atom characterising a random mixture with the same atomic content. The moments of the Ni atoms in all calculations, including the *ab initio* studies, are significantly smaller than the moments of pure fcc Ni (0.575 μ_B in MCE simulations; 0.605 μ_B according to the experimental data [22]). Ni moments are aligned ferromagnetically with respect to the Fe moments. Magnetic moments of ordered Fe_2CrNi alloy, as well as each of its components, are plotted in Figure 7 as functions of temperature. The alloy remains magnetic until very high temperatures. Simulations performed using the current MCE Hamiltonian predict the Curie temperature close to 1050-1100 K, which is slightly higher than the value of $\sim$ 1000 K found using the previous fit [4]. The effect of transition temperature increase compared to pure Ni and binary FeNi and $FeNi_3$ alloys is similar to the one observed for fcc Fe-Ni, where the chemically ordered $FeNi_3$ compound has a higher Curie temperature than pure Ni. In relation to the ternary Fe_2CrNi alloy, we again attribute the high stability of its magnetically ordered configuration to strong antiferromagnetic coupling between Fe and Cr atoms.

V. Conclusions

This paper describes an application of Magnetic Cluster Expansion to a ternary alloy. We chose a technologically relevant Fe-Ni-Cr fcc alloy as a subject of this initial study. Despite the fact that parameterization of MCE model involves several fairly strong approximations, for example the model neglects the environmental dependence of the Landau on-site terms, our low temperature predictions agree very well with DFT data. We are also able to explore high temperature magnetic properties of the alloys, by performing Monte Carlo simulations for both random and ordered alloy configurations. Strong antiferromagnetic Fe-Cr interactions give rise to the fact that chromium atoms prefer to substitute Ni positions in all the ordered Fe-Ni compounds. The replacement of Ni atoms by Cr also increases the Curie temperature of Fe-rich ordered alloys. Interplay between chemical and magnetic degrees of freedom is responsible for the very high Curie temperature of ordered Fe_2CrNi alloys, similar to the case of bcc Fe-Cr alloys [20]. The MCE predictions agree very well with the available experimental data and *ab initio*

calculations performed within collinear magnetic scheme [3], showing that MCE Hamiltonian-based Monte Carlo simulations can be successfully applied to complex ternary magnetic alloys that exhibit ferromagnetic and antiferromagnetic properties. A future improvement of MCE parametrization for multi-component magnetic alloys can be achieved by using more efficient and larger ab-initio data base within constrained non-collinear magnetic formalism [29].

This work was part-funded by the EuroFusion Consortium, and has received funding from Euratom research and training programme 2014-2018 under grant agreement number No 633053, and funding from the RCUK Energy Programme (Grant Number EP/I501045). The views and opinions expressed herein do not necessarily reflect those of the European Commission. To obtain further information on the data and models underlying this paper please contact PublicationsManager@ccfe.ac.uk. This work was also part-funded by the United Kingdom Engineering and Physical Sciences Research Council via a programme grant EP/G050031. This work was also partly funded by the Accelerated Metallurgy Project, which is co-funded by the European Commission in the 7th Framework Programme (Contract NMP4-LA-2011-263206), by the European Space Agency and by the individual partner organizations.

References

1. T. Toyama, Y. Nozawa, W. Van Renterghem, Y. Matsukawa, M. Hatakeyama, Y. Nagai, A. Al Mazouzi, and S. Van Dyck, *J. Nucl. Mater.* **425**, 71 (2012).
2. A.-A.F. Tavassoli, E. Diegele, R. Lindau, N. Luzginova, and H. Tanigawa, *J. Nucl. Mater.* **455**, 269 (2014).
3. M. Yu. Lavrentiev, J. S. Wróbel, D. Nguyen-Manh, and S. L. Dudarev, *Phys. Chem. Chem. Phys*. **16**, 16049 (2014).
4. J. S. Wróbel, D. Nguyen-Manh, M. Yu. Lavrentiev, M. Muzyk, and S. L. Dudarev, *Phys. Rev. B* **91**, 024108 (2015).
5. M. Yu. Lavrentiev, D. Nguyen-Manh, and S. L. Dudarev, *Phys. Rev. B* **81**, 184202 (2010).
6. M. Yu. Lavrentiev, S. L. Dudarev, and D. Nguyen-Manh, *J. Nucl. Mater.* **386-388**, 22 (2009).
7. M. Yu. Lavrentiev, D. Nguyen-Manh, and S. L. Dudarev, *Comput. Mater. Sci*. **49**, S199 (2010).
8. D. Terentyev and A. Bakaev, *J. Nucl. Mater.* **442**, 208 (2013).
9. A.R. Farinha, B. Tavares, R. Mendes, and M. T. Vieira, *J. Alloys Compd.* **536S**, S575 (2012).
10. G.R. Odette, M.J. Alinger, and B.D.Wirth, *Annu. Rev. Mater. Res.* **38**, 471 (2008).
11. V. I. Gomankov, I. M. Puzei, and V. N. Sigaev, *Pisma Zh. Eksp. Teor. Fiz.* **13**, 600 (1971).

12. A. Z. Menshikov, V. Y. Arkhipov, A. I. Zakharov, and S. K. Sidorov, *Fiz. Met. Metalloved.* **34**, 309 (1972).

13. P. Cenedese, F. Bley, and S. Lefebvre, *Acta Cryst.* **A40**, 228 (1984).

14. I. Mirebeau, M. Hennion, and G. Parette, *Phys. Rev. Lett.* **53**, 687 (1984).

15. B. Schönfeld, L. Reinhard, G. Kostorz, and W. Buhrer, *Phys. Stat. Sol. B* **148**, 457 (1988).

16. R. Caudron, M. Sarfati, M. Barrachin, A. Finel, F. Ducastelle, and F. Solal, *J. Phys. I France* **2**, 1145 (1992).

17. A. Z. Menshikov, C. Dimitrov, and A. E. Teplykh, *J. Phys. III France* **7**, 1899 (1997).

18. J. L. Robertson, G. E. Ice, C. J. Sparks, X. Jiang, P. Zschack, F. Bley, S. Lefebvre, and M. Bessiere, *Phys. Rev. Lett.* **82**, 2911 (1999).

19. Y. Tsunoda, *J. Phys.: Condens. Matter* **1**, 10427 (1989).

20. A. Onodera, Y. Tsunoda, N. Kunitomi, O. A. Pringle, R. M. Nicklow, and R. M. Moon, *Phys. Rev. B* **50**, 3532 (1994).

21. H. P. J. Wijn, ed., *Magnetic Properties of Metals*, Landolt-Börstein. Numerical Data and Functional Relationships in Science and Technology, Vol. 19 (Springer, Berlin, Heidelberg, 1991).

22. S. Blundell, *Magnetism in Condensed Matter*, Oxford University Press (2001).

23. M. Yu. Lavrentiev, K. Mergia, M. Gjoka, D. Nguyen-Manh, G. Apostolopoulos, and S. L. Dudarev, *J. Phys.: Condens. Matter* **24**, 326001 (2012).

24. J. F. Albertsen, G. B. Jensen, and J. M. Knudsen, *Nature* **273**, 453 (1978).

25. R. S. Clarke Jr., and E. R. D. Scott, *Am. Mineral.* **65**, 624 (1980).

26. C.-W. Yang, D. B. Williams, and J. I. Goldstein, *Geochim. Cosmochim. Acta* **61**, 2943 (1997).

27. W. Xiong, P. Hedström, M. Selleby, J. Odqvist, M. Thuvander, and Q. Chen, *CALPHAD* **35**, 355 (2011).

28. C. Bansal and G. Chandra, *Solid State Commun.* **19**, 107 (1976).

29. D. Nguyen-Manh, P.-W. Ma, M. Yu. Lavrentiev, and S.L. Dudarev, *Ann. Nuclear Energy* **77**, 246 (2015).

Table 1. Non-magnetic interaction parameters I_{ij} and magnetic Heisenberg interaction parameters Y_{ij} (meV) derived using a fitting procedure described in [3].

	1st NN		2nd NN		3rd NN		4th NN	
	I_{ij}	Y_{ij}	I_{ij}	Y_{ij}	I_{ij}	Y_{ij}	I_{ij}	Y_{ij}
Fe-Fe	1.856364	-0.793072	10.741989	-10.827175	-0.405778	0.546719	-2.047610	2.305911
Fe-Ni	-2.710858	-3.805516	-12.447877	-1.487362	0.131012	-0.530692	-3.104198	0.136000
Fe-Cr	-6.627640	5.778819	-4.571750	0.488416	-4.791461	-0.309644	6.560627	-0.366602
Ni-Ni	1.132506	-13.153009	0.006062	7.227536	11.972890	-5.604799	2.557930	-6.744045
Ni-Cr	-0.419121	-5.501130	7.440212	0.692985	-11.923519	-0.820111	-7.328073	-0.629514
Cr-Cr	-3.933508	-0.741406	-4.550795	-0.011726	-4.898933	0.416839	2.322535	0.296039

Table 2. The on-site Landau expansion terms (in meV units) entering the MCE Hamiltonian (1).

	Fe	Ni	Cr
A	-0.99016	30.37460	-3.47938
B	29.05331	455.69	5.226
C	-6.49401	-138.05	
D	0.42817	18.8	

Table 3. Magnetic moments per atom computed for several SQS structures using the Magnetic Cluster Expansion model (with and without the collinearity constraint) and DFT (μ_B).

		MCE (non-collinear)	MCE (collinear)	DFT
1	M_{total}	0.674	1.221	1.147
	M_{Fe}	1.244	2.202	2.016
	M_{Ni}	0.294	0.415	0.336
	M_{Cr}	1.372	2.155	1.776
2	M_{total}	0.727	1.154	1.123
	M_{Fe}	1.211	2.081	1.957
	M_{Ni}	0.331	0.433	0.348
	M_{Cr}	0.942	2.060	1.682
3	M_{total}	0.493	0.386	1.159
	M_{Fe}	0.919	0.932	2.036
	M_{Ni}	0.224	0.041	0.321
	M_{Cr}	1.040	1.433	1.585
4	M_{total}	0.836	1.124	1.045
	M_{Fe}	1.600	2.111	1.844
	M_{Ni}	0.422	0.454	0.399
	M_{Cr}	1.748	2.142	1.530
5	M_{total}	0.641	1.200	1.115
	M_{Fe}	1.185	2.222	1.952
	M_{Ni}	0.332	0.436	0.397
	M_{Cr}	1.185	2.136	1.557

Table 4. Magnetic moments per atom computed for the ground states of random (without and with the collinearity constraint) and ordered Fe_2NiCr system using the Magnetic Cluster Expansion model and for the ordered Fe_2NiCr using DFT [4] (μ_B).

	Random		Ordered	
	Non-collinear MCE	Collinear MCE	MCE (collinear)	DFT [4]
M_{total}	0.025	0.206	0.921	0.471
M_{Fe}	0.072	0.552	2.715	2.085
M_{Ni}	0.013	0.130	0.381	0.152
M_{Cr}	0.056	0.410	2.131	2.437

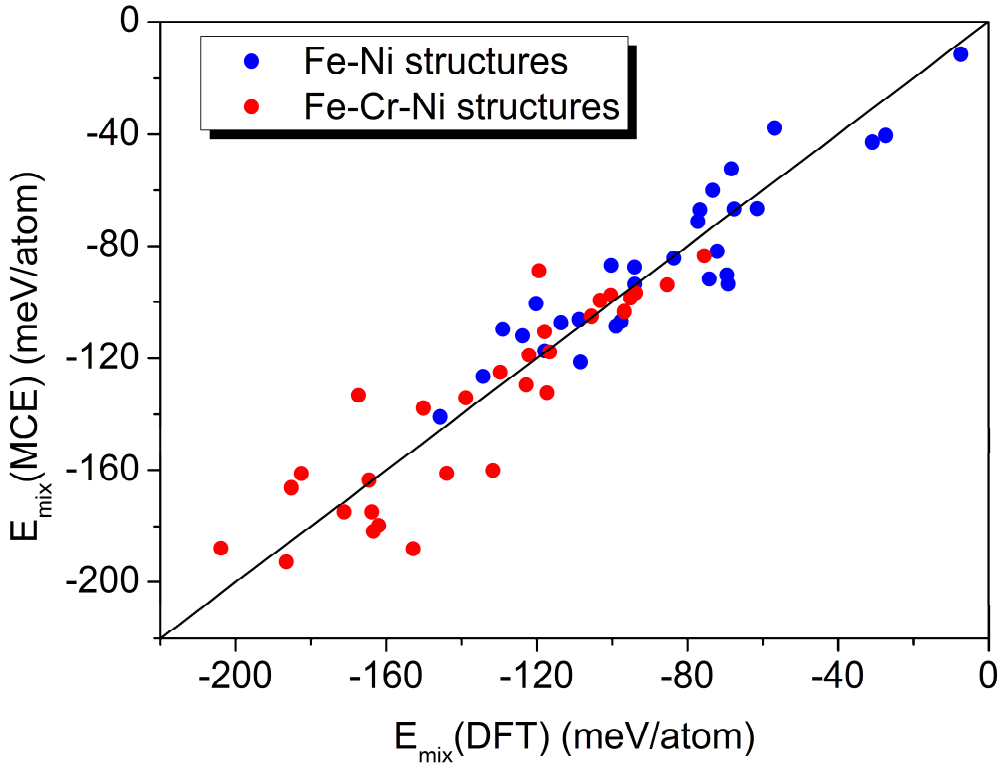

Figure 1. Comparison between DFT and MCE energies of mixing for alloy configurations used for fitting the MCE Hamiltonian. Data points for Fe-Ni and Fe-Cr-Ni alloys are shown using different colours.

Figure 2. Magnetic moment of random Fe-Ni-Cr mixture (μ_B) without (a) and with (b) collinearity constraint applied.

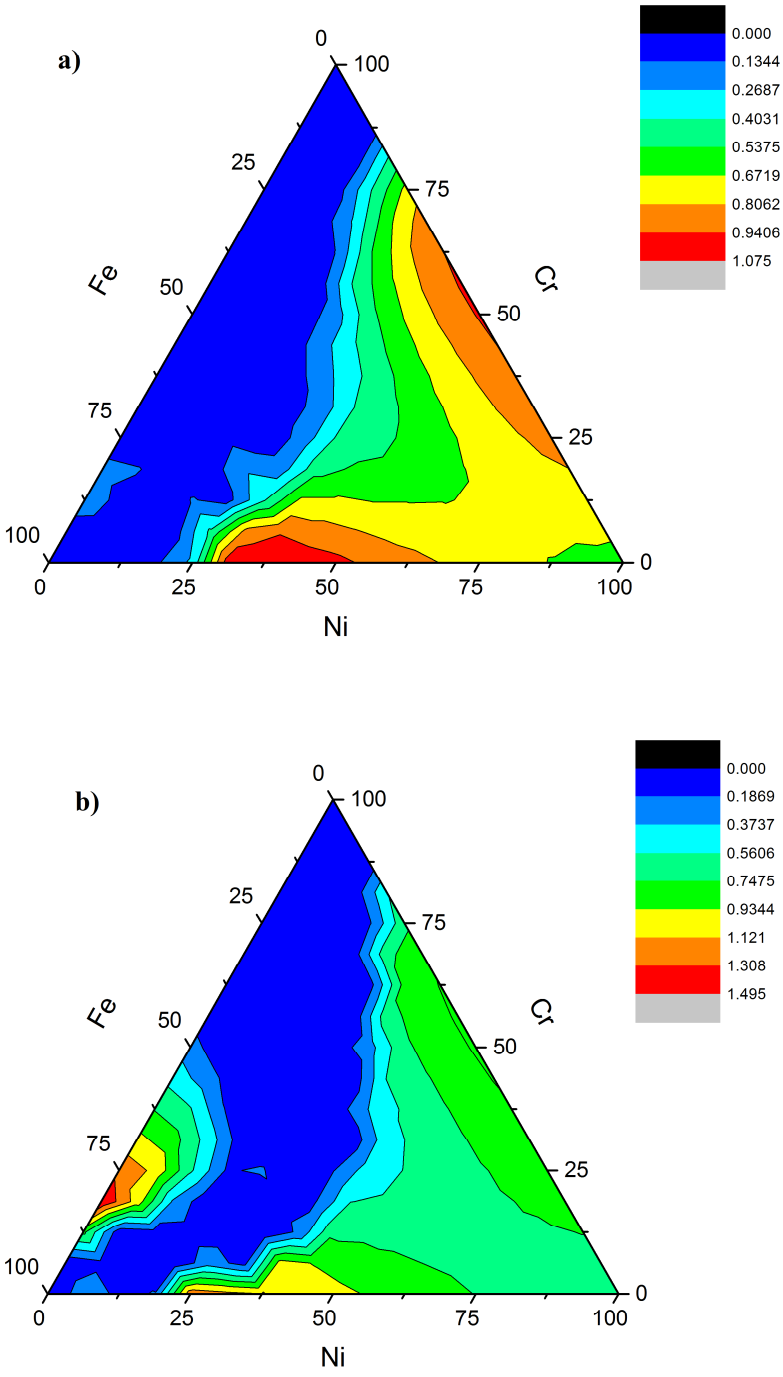

Figure 3. Enthalpy of mixing (a) and the formation enthalpy (b) of random Fe-Ni-Cr mixtures (meV/atom) simulated with no collinearity constraint applied.

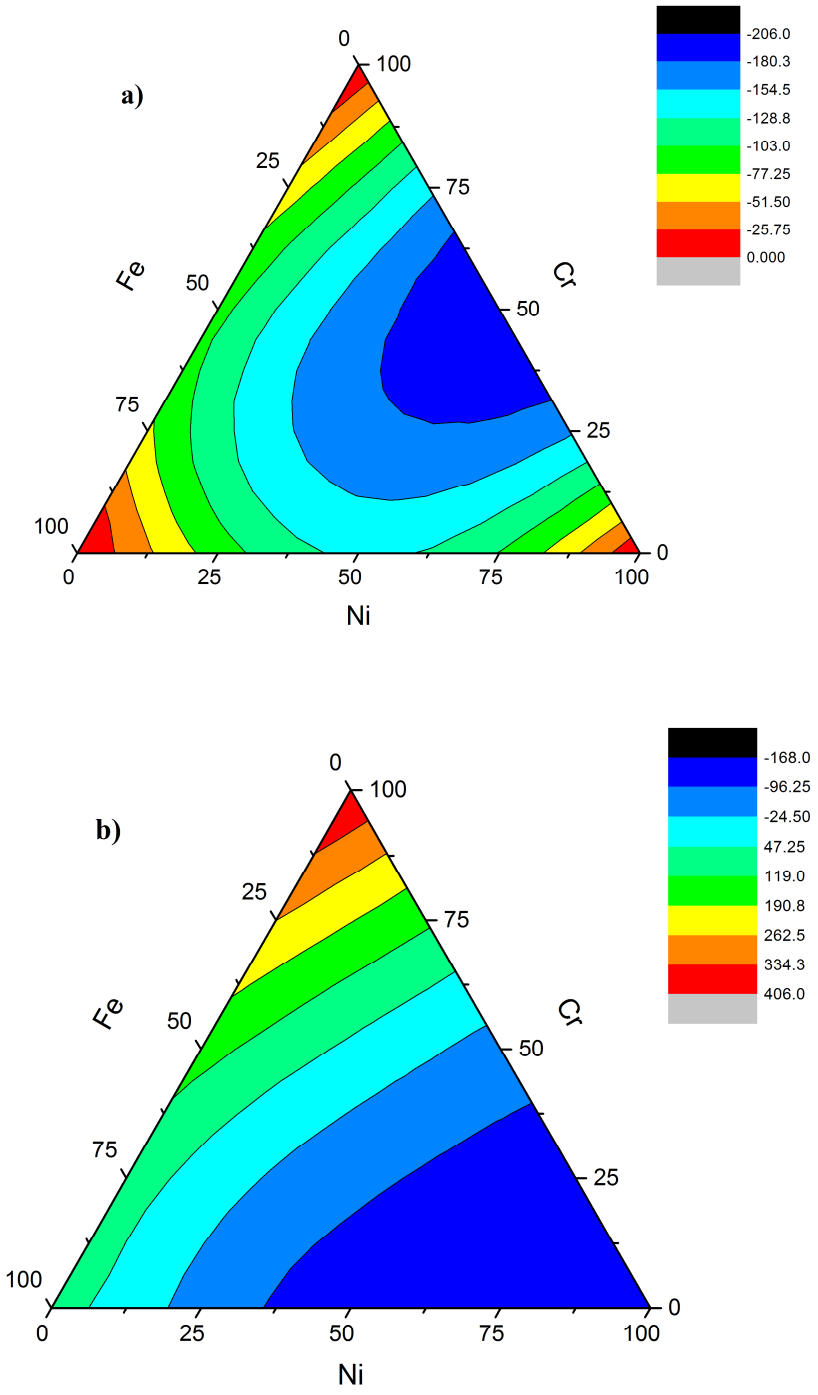

Figure 4. Magnetic moment of random Fe-Ni-Cr mixtures (μ_B) at T=500 K.

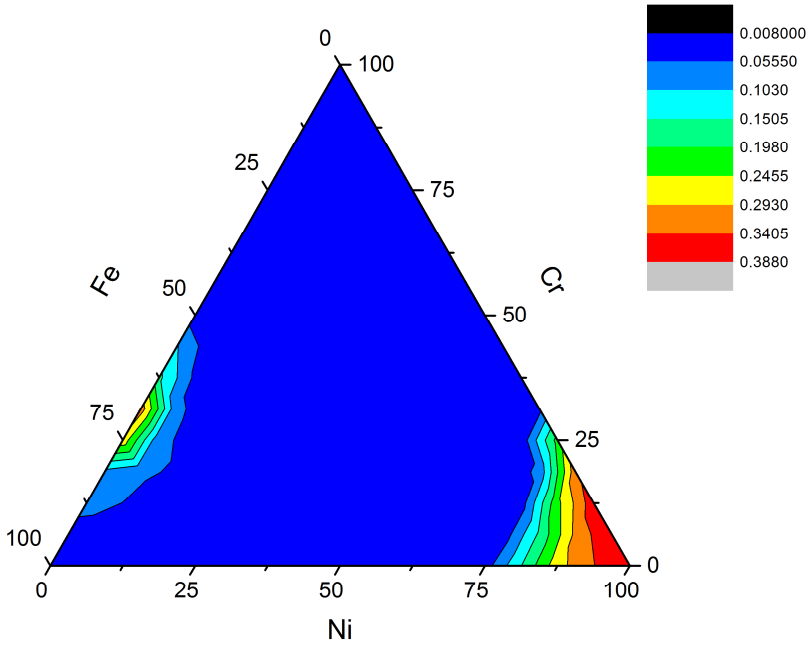

Figure 5. Energy of ordered Fe-Ni fcc structures with randomly distributed Cr replacing Fe, Ni, or both Fe and Ni atoms. The curves refer to the following ordered alloy structures: Fe_3Ni $L1_2$ (a), FeNi $L1_0$ (b), $FeNi_3$ $L1_2$ (c).

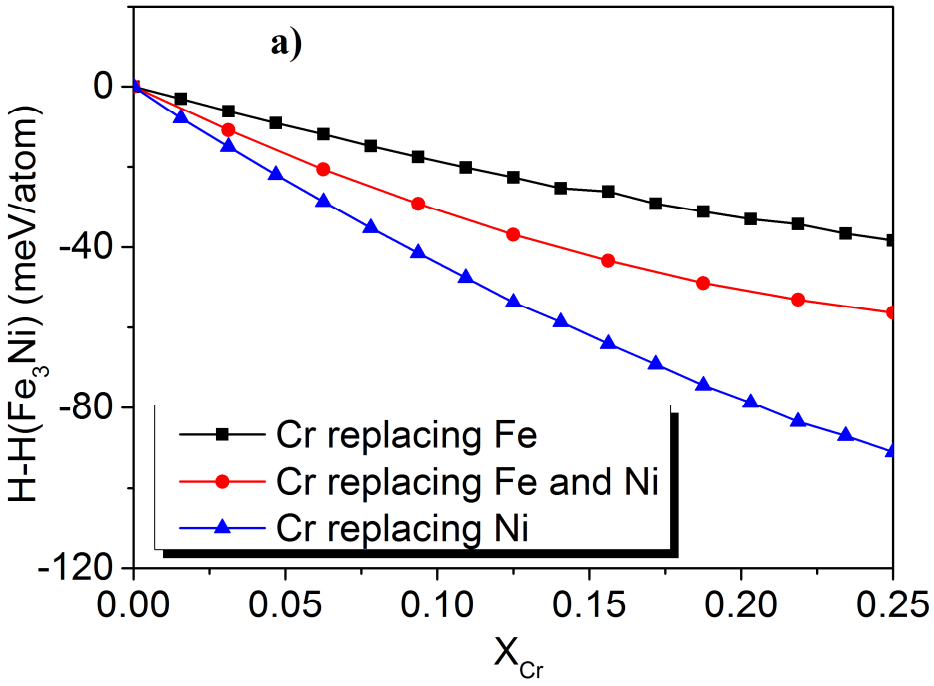

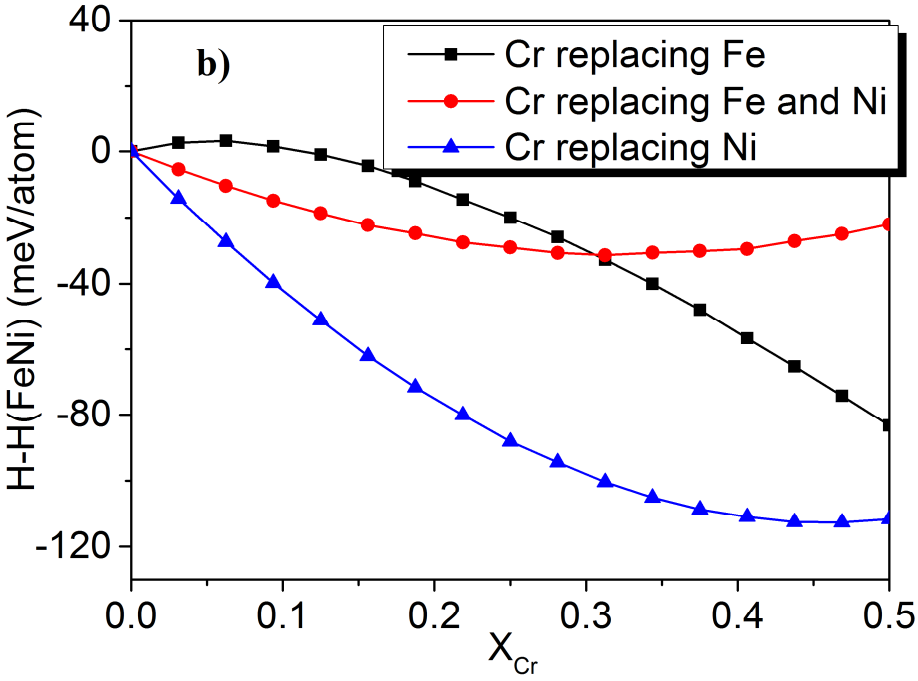
b)
Cr replacing Fe
Cr replacing Fe and Ni
Cr replacing Ni
H-H(FeNi) (meV/atom)
40
0
-40
-80
-120
0.0
0.1
0.2
0.3
0.4
0.5
X_Cr

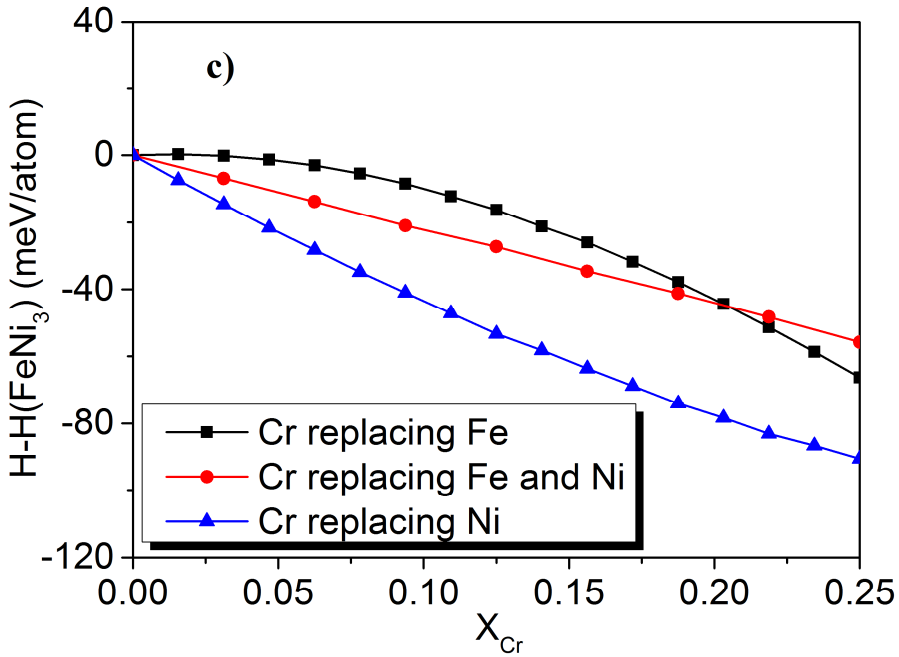
c)
Cr replacing Fe
Cr replacing Fe and Ni
Cr replacing Ni
H-H(FeNi3) (meV/atom)
40
0
-40
-80
-120
0.00
0.05
0.10
0.15
0.20
0.25
X_Cr

Figure 6. Magnetic moments of ordered Fe-Ni fcc alloys containing randomly distributed 6.25 at. % Cr atoms replacing Fe, Ni, or both Fe and Ni atoms. The curves refer to the alloy structures as follows: Fe_3Ni $L1_2$ (a), FeNi $L1_0$ (b), $FeNi_3$ $L1_2$ (c). The moments computed for ordered Fe-Ni alloys with no Cr present are shown for comparison.

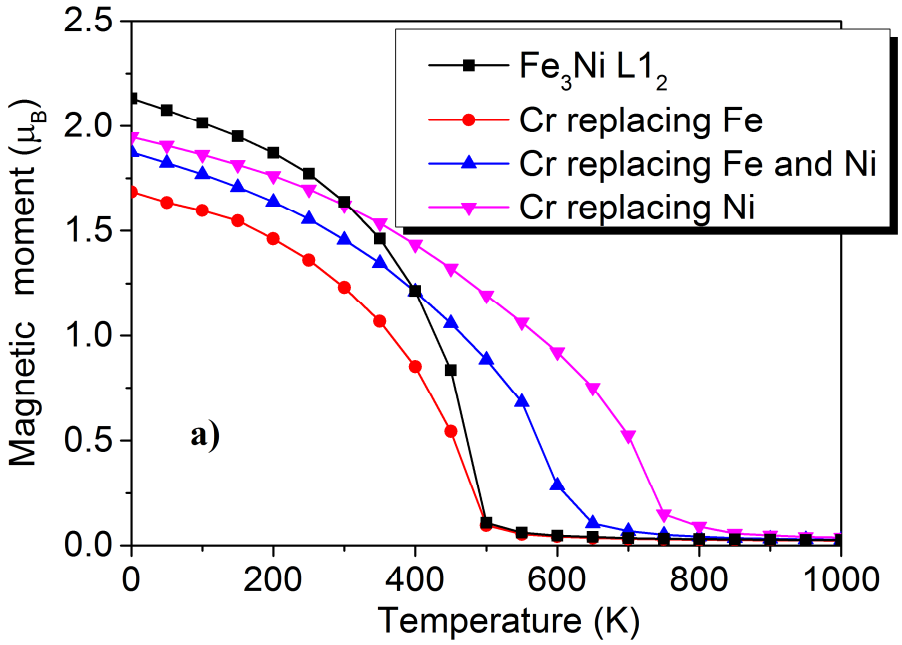

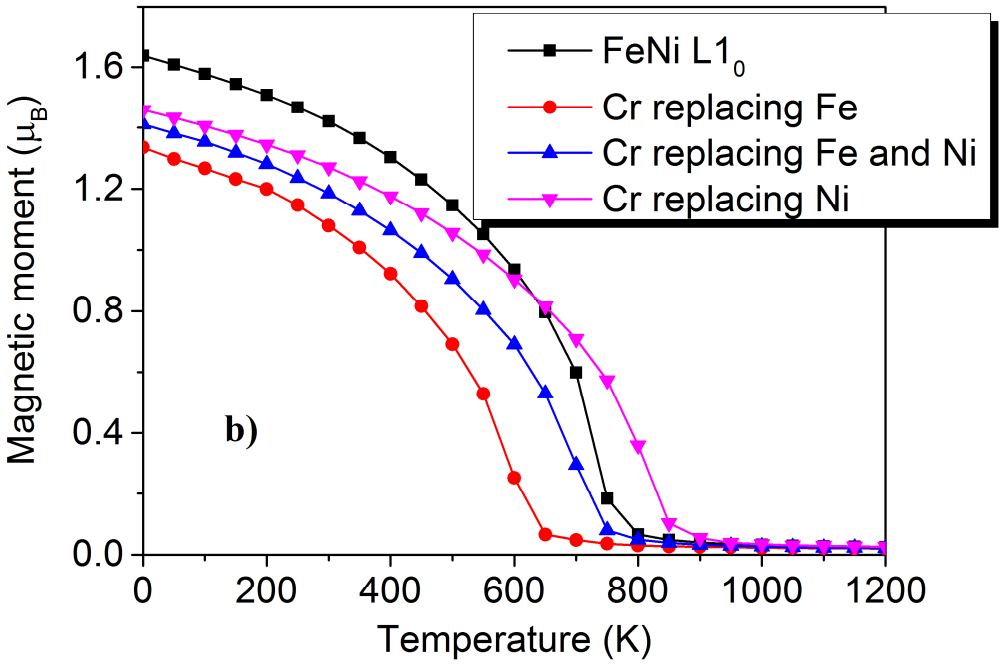
FeNi L1$_0$
Cr replacing Fe
Cr replacing Fe and Ni
Cr replacing Ni
b)
Magnetic moment (μ_B)
Temperature (K)
0.0
0.4
0.8
1.2
1.6
0
200
400
600
800
1000
1200

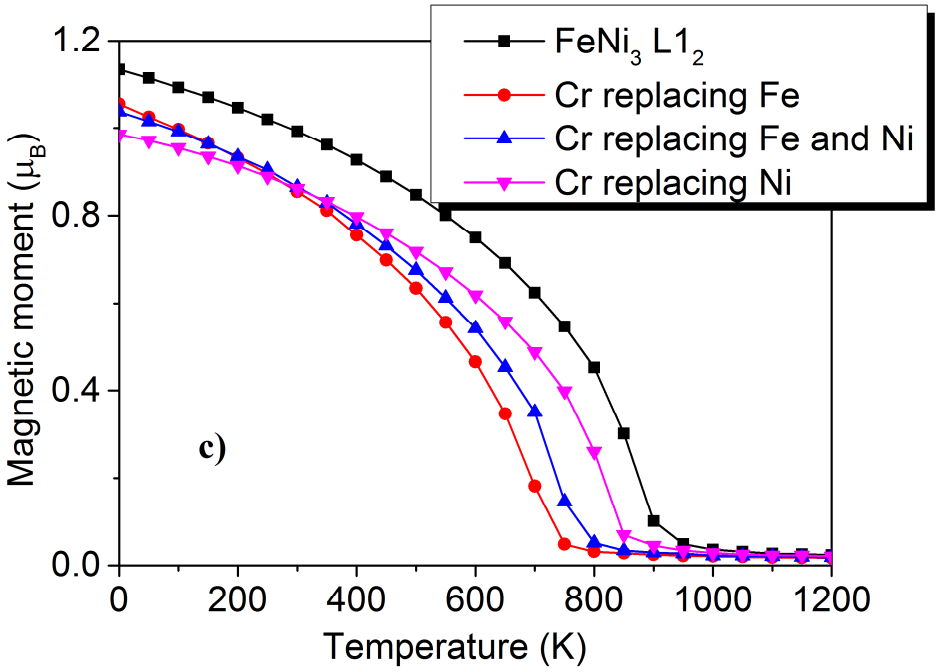
FeNi$_3$ L1$_2$
Cr replacing Fe
Cr replacing Fe and Ni
Cr replacing Ni
c)
Magnetic moment (μ_B)
Temperature (K)
0.0
0.4
0.8
1.2
0
200
400
600
800
1000
1200

Figure 7. Temperature dependence of the total magnetic moment of ordered Fe_2CrNi alloy, and the moments of atoms forming the alloy.